Mon. Not. R. Astron. Soc. **421,** 202–212 (2012) doi:10.1111/j.1365-2966.2012.20291.x

Two new young, wide, magnetic + non-magnetic double-degenerate binary systems

P. D. Dobbie,[1⋆] R. Baxter,[2] B. Külebi,[3] Q. A. Parker,[1,2] D. Koester,[4] S. Jordan,[5] N. Lodieu[6,7] and F. Euchner[8]

[1]*Australian Astronomical Observatory, PO Box 296, Epping, NSW, 1710, Australia*
[2]*Department of Physics & Astronomy, Macquarie University, NSW, 2109, Australia*
[3]*Institut de Ciències de l'Espai (CSIC-IEEC), Facultat de Ciències, Campus UAB, Torre C5-parell, 2ª planta, 08193 Bellaterra, Spain*
[4]*Institut für Theoretische Physik und Astrophysik, University of Kiel, 24098 Kiel, Germany*
[5]*Astronomisches Rechen-Institut, Zentrum für Astronomieder Universität Heidelberg, Mönchhofstrasse 1214, D-69120 Heidelberg, Germany*
[6]*Instituto de Astrofísica de Canarias, Vía Láctea s/n, E-38200 La Laguna, Tenerife, Spain*
[7]*Departmento de Astrofísica, Universidad de La Laguna, E-38205 La Laguna, Tenerife, Spain*
[8]*Swiss Seismological Service, ETH Zurich, Schafmattstrasse 30, HPP P3, 8093 Zurich, Switzerland*

Accepted 2011 November 29. Received 2011 November 28; in original form 2011 September 4

ABSTRACT

We report the discovery of two, new, rare, wide, double-degenerate binaries that each contain a magnetic and a non-magnetic star. The components of SDSS J092646.88+132134.5 + J092647.00+132138.4 and of SDSS J150746.48+521002.1 + J150746.80+520958.0 have angular separations of only 4.6 arcsec ($a \sim 650$ au) and 5.1 arcsec ($a \sim 750$ au), respectively. They also appear to share common proper motions. Follow-up optical spectroscopy has revealed each system to consist of a DA and a H-rich high-field magnetic white dwarf (HFMWD). Our measurements of the effective temperatures and the surface gravities of the DA components reveal both to have larger masses than is typical of field white dwarfs. By assuming that these degenerates have evolved essentially as single stars, owing to their wide orbital separations, we can use them to place limits on the total ages of the stellar systems. These suggest that in each case the HFMWD is probably associated with an early-type progenitor ($M_{\rm init} > 2\,{\rm M}_{\odot}$). We find that the cooling time of SDSS J150746.80+520958.0 (DAH) is lower than might be expected had it followed the evolutionary path of a typical single star. This mild discord is in the same sense as that observed for two of the small number of other HFMWDs for which progenitor mass estimates have been made, RE J0317-853 and EG 59. The mass of the other DAH, SDSS J092646.88+132134.5, appears to be smaller than expected on the basis of single-star evolution. If this object was/is a member of a hierarchical triple system it may have experienced greater mass loss during an earlier phase of its life as a result of its having a close companion. The large uncertainties on our estimates of the parameters of the HFMWDs suggest that a larger sample of these objects is required to firmly identify any trends in their inferred cooling times and progenitor masses. This should shed further light on their formation and on the impact magnetic fields have on the late stages of stellar evolution. To serve as a starting point, we highlight two further candidate young, wide magnetic + non-magnetic double-degenerate systems within SDSS, CBS 229 and SDSS J074853.07+302543.5 + J074852.95+302543.4, which should be subjected to detailed (resolved) spectroscopic follow-up studies.

Key words: binaries:general – stars: magnetic fields – white dwarfs.

1 INTRODUCTION

A non-negligible proportion of white dwarfs appear to possess substantial magnetic fields, with strengths typically >1 MG. A number of studies have determined that they represent between ∼5 and 15 per cent of the white dwarf population, but their origins remain

⋆E-mail: pdd@aao.gov.au

unclear (Angel, Borra & Landstreet 1981; Liebert, Bergeron & Holberg 2003; Kawka et al. 2007; Külebi et al. 2009). They are often referred to as high-field magnetic white dwarfs (HFMWDs, e.g. Wickramasinghe & Ferrario 2005). While the mass distribution of field white dwarfs is found to be strongly peaked around $0.6\,M_{\odot}$ (e.g. Liebert, Bergeron & Holberg 2005a; Koester et al. 2009), the mass distribution of the HFMWDs is flatter and skewed towards higher masses, $M \sim 0.9\,M_{\odot}$ (e.g. Liebert et al. 2003). Three of the 10 ultramassive ($M > 1.1\,M_{\odot}$) white dwarfs identified in the extreme ultraviolet surveys appear to be HFMWDs (Vennes, Ferrario & Wickramasinghe 1999).

At present, there are two principal theories regarding their formation. In the 'fossil field' hypothesis, the HFMWDs are the descendants of Ap + Bp stars, a magnetic, chemically peculiar subset of objects with spectral types ranging from late-B to early-F (Angel et al. 1981). This is in accord with the similar magnetic fluxes of the HFMWDs and Ap + Bp stars and with the predicted long decay times of the fields in these objects. Moreover, the higher average mass of the HFMWDs is explained naturally here as a result of the form of the stellar initial–final mass relation (IFMR), a positive correlation between the main-sequence masses of stars and their white dwarf remnant masses (e.g. Weidemann 2000). However, in light of more recent results, the proportion of late-B to early-F stars that can be classified as Ap + Bp may be too low by a factor of 2–3 to be consistent with the larger revised estimates of the percentage of HFMWDs in the general white dwarf population (e.g. Kawka et al. 2003). To alleviate this apparent shortfall in progenitors, it is required that ∼40 per cent of stars with $M > 4.5\,M_{\odot}$ also evolve to become HFMWDs (e.g. Wickramasinghe & Ferrario 2005).

Alternatively, Tout et al. (2008) have proposed that the magnetic fields of HFMWDs are generated by differential rotation within the common envelope gas that engulfs a primordial close binary system when the primary star expands to giant dimensions and overfills its Roche lobe. An isolated HFMWD is predicted to form if the cores of the components merge before this envelope is dispersed. However, if the gas is removed prior to this, the outcome is instead expected to be a magnetic cataclysmic variable. This hypothesis can account for the puzzling lack of detached HFMWD + late-type star binary systems that has emerged from the Sloan Digital Sky Survey (SDSS; e.g. Liebert et al. 2005b). It might also explain the reported discrepancies in the cooling times of the small number of HFMWDs that it has been possible to test against evolutionary models for single stars (e.g. RE J0317-835 and EG59, Barstow et al. 1995; Ferrario et al. 1997; Claver et al. 2001; Casewell et al. 2009).

The identification of new HFMWDs for which there is the opportunity to set constraints on their masses, cooling times and the ages of their parent populations can further address questions regarding their origins. Traditionally, white dwarf members of open clusters are used, as their masses can be constrained from their observed fluxes using a mass–radius relation (e.g. Casewell et al. 2009). Subsequently, their cooling times can be derived and compared with those of the non-magnetic degenerate members for which progenitor masses can be estimated straightforwardly. Unfortunately, fewer than a handful of HFMWDs have been found in open clusters to date. These have tended to be faint, owing to their substantial distances (e.g. NGC 6819-8, $V \approx 23.0$, Kalirai et al. 2008), and thus they are not particularly amenable to detailed follow-up study.

An alternative approach focuses on field HFMWDs in nearby, wide, double-degenerate systems in which the components are sufficiently far apart to have evolved essentially as separate entities but the system age and distance can be determined from the non-magnetic companion star (e.g. Girven et al. 2010). However, only two of these spatially resolved binaries have been identified to date. RE J0317-853 (Barstow et al. 1995), at $d \sim 30$ pc (Külebi et al. 2010), was discovered in the course of the extreme-ultraviolet all-sky surveys undertaken with the *Röntgensatellit* (e.g. Pye et al. 1995) and the *Extreme Ultraviolet Explorer* (e.g. Bowyer et al. 1996) satellites. It consists of a common proper motion pairing of a $\sim 0.85\,M_{\odot}$ DA and an ultramassive HFMWD with a field strength of $B \sim 450$ MG (Ferrario et al. 1997; Burleigh, Jordan & Schweizer 1999) that are separated on the sky by 7 arcsec. The more recently discovered common proper motion system PG 1258+593 + SDSS J130033.48+590407.0 (Girven et al. 2010) contains a pair of near-equal-mass ($M \approx 0.54\,M_{\odot}$) hydrogen-rich white dwarfs that are separated on the sky by 16 arcsec. The HFMWD component, which has a field strength of $B \sim 6$ MG, is the cooler of the pair. In addition, three unresolved double-degenerate systems containing a magnetic and a non-magnetic object are also currently listed in the refereed literature. LB 11146 (Liebert et al. 1993) is known to be a physically close system (Nelan 2007), while the orbital separations of the white dwarfs in RE J1439+75 (Vennes et al. 1999) and G 62-46 (Bergeron, Ruiz & Leggett 1993) might also be relatively small.

With several large-area charged-coupled device (CCD) imaging surveys such as SDSS (York et al. 2000), VST ATLAS (http://www.astro.dur.ac.uk/Cosmology/vstatlas/) and SkyMapper (Keller et al. 2007) having recently been completed or soon to be undertaken, the prospects for unearthing more young, wide, magnetic + non-magnetic white dwarf binaries are excellent. Here we report the discovery and confirmation of two further examples of such systems, SDSS J092646.88+132134.5 + J092647.00+132138.4 (hereafter System 1) and SDSS J150746.48+521002.1 + J150746.80+520958.0 (hereafter System 2). In the following sections we briefly describe our broader survey for wide double-degenerate binaries and demonstrate that the components of these two new pairings share common proper motions. We perform a spectroscopic analysis of the two white dwarfs in each system to assess their masses and cooling times. Subsequently, we examine the objects in the context of canonical single-star evolutionary theory and place constraints on the nature of the progenitors of the HFMWDs. In addition, we search for evidence that these white dwarfs have more exotic formation histories. We finish by highlighting two further candidate wide, magnetic + non-magnetic double-degenerate binaries that may be suitable for this type of analysis. These could serve as a starting point for the construction of an enlarged sample of these systems, which will be necessary for a better understanding of the formation of HFMWDs.

2 DISCOVERY OF YOUNG, WIDE, MAGNETIC + NON-MAGNETIC WHITE DWARF BINARIES

2.1 Imaging search for wide, double-degenerate systems

We have been conducting a survey for young, wide, double-degenerates using imaging and spectroscopic data from the SDSS. The full details of this study will be described in a forthcoming paper (Baxter et al. in prep.) but we provide a brief outline of our approach here so that this result can be placed in context. We selected from DR7 (the 7th SDSS data release) all point sources flagged as photometrically clean with $r \leq 20.0, u - g \leq 0.5, g - r \leq 0.0$ and $r - i < 0.0$ (corresponding to white dwarfs with $T_{\rm eff} \gtrsim 9000$ K, e.g. Eisenstein et al. 2006) that have another object satisfying these colour–magnitude criteria within 30 arcsec. The resulting candidate systems were visually inspected using the SDSS

Table 1. A summary of the photometric and astrometric properties of the components of our two putative wide double-degenerate systems.

IAU	Name	u	g	r	i	z	$\mu_\alpha \cos\delta$	μ_δ
				SDSS			(mas yr^{-1})	
SDSS J092646.88+132134.5	DAH1	18.46 ± 0.02	18.34 ± 0.02	18.39 ± 0.01	18.50 ± 0.02	18.60 ± 0.03	-8.6 ± 6.9	-77.2 ± 9.6
SDSS J092647.00+132138.4	DA1	18.74 ± 0.03	18.40 ± 0.03	18.46 ± 0.05	18.60 ± 0.04	18.79 ± 0.03	-11.6 ± 6.9	-65.3 ± 9.6
SDSS J150746.48+521002.1	DA2	17.14 ± 0.02	16.91 ± 0.03	17.29 ± 0.01	17.55 ± 0.02	17.84 ± 0.02	-30.3 ± 4.9	$+12.7 \pm 5.8$
SDSS J150746.80+520958.0	DAH2	17.98 ± 0.03	17.76 ± 0.03	18.06 ± 0.01	18.33 ± 0.02	18.55 ± 0.03	-31.0 ± 4.9	$+13.1 \pm 5.8$

finder chart tool to weed out a number of spurious pairings (e.g. blue point-like detections within resolved galaxies). This procedure led to the identification of 52 candidate systems, including the previously known double-degenerate binaries PG 0922+162 (Finley & Koester 1997) and HS 2240+1234 (Jordan et al. 1998). The associated SDSS spectroscopy, which is available for 21 objects in 19 of these pairs, reveals 17 DAs, 1 DB and 3 DCs but no quasars or subdwarfs, suggesting that contamination levels in this sample are low. We have obtained long-slit spectroscopic follow-up data for 13 additional candidate binaries to date and all have turned out to be composed of white dwarfs, confirming the low level of contamination.

Of the 13 pairings, System 1 and System 2 both appear to harbour a HFMWD. Their components are separated on the sky by only 4.35 and 5.05 arcsec, respectively. Their u, g, r, i and z magnitudes are listed in Table 1. To ascertain the likelihood of chance alignments we used equation (1) (Struve 1852), under the assumption of a random on-sky distribution of objects, where N is the number of sources satisfying the photometric selection criteria in area A (square degrees) and ρ is the maximum projected separation (degrees):

$$n(\leq \rho) = N(N-1)\pi\rho^2/2A. \quad (1)$$

We estimate $n(4 < \rho \leq 6\,\mathrm{arcsec}) \sim 0.3$ for $N = 36\,231$ and $A = 11\,663$ square degrees. In the course of our survey we unearthed a total of 10 pairs of objects with separations in this range, suggesting that the probability of any one being a mere chance alignment is $P \sim 0.03$.

2.2 Astrometric follow-up and proper motions

To probe the reality of the putative associations between the two sources in each of these pairs, we examined their relative proper motions. We note that Girven et al. (2010) used proper motions to confirm the association of PG 1258+593 + SDSS J130033.48+590407.0 in their recent exploration of the bottom end of the IFMR. In principle, measurements of this nature can be obtained from one of a number of online data bases featuring imaging of widely separated epochs, for example the United States Naval Observatory B1.0 catalogue (USNO-B1.0; Monet et al. 2003), SDSS (e.g. Munn et al. 2004), the SuperCOSMOS Sky Survey (SSS; Hambly et al. 2001) and the extended Position and Proper Motion catalogue (PPMXL; Roeser, Demleitner & Schilbach 2010). However, these resources rely heavily on comparatively low-spatial-resolution photographic plate exposures. Examination of the values reported in these catalogues indicates that the small separations of the components of our candidate binaries have compromised their accuracy. For example, the astrometry reported in the PPMXL catalogue suggests that the relative positions of the objects in these two pairs should have changed by several arcseconds in the ∼50 years between the imaging of the first Palomar Sky Survey and SDSS. However, visual inspection of these data reveals no discernable difference. Therefore, we opted to perform our own astrometric measurements of System 1 and System 2. For the first system we adopted the g-band data from SDSS (2006 January 6) and a B-band acquisition frame (2010 February 6) from our spectroscopic follow-up program on the European Southern Observatory (ESO) Very Large Telescope (VLT) as first and second epoch images respectively. We used (SExtractor; Bertin & Arnouts 1996) to determine the positions of ∼10 unblended, stellar-like objects lying in close proximity to the candidate white dwarfs. As no suitable second CCD image of System 2 was available to us we resorted to using data from the first Palomar Sky Survey (Plate 2376 observed on 1954 June 28) and the SDSS r-band imaging (2002 June 9) as our first and second epoch images of this system, respectively. Here we determined the positions of unsaturated stellar-like objects lying within a few arcminutes of the candidate white dwarfs. In detecting these stars and determining their centroids in the photographic data, no smoothing filter was applied to the image (in order to minimize blending of the stellar profiles), and only those pixels substantially above the background ($\gtrsim 5\sigma$) were included in the calculations.

For each pair of objects we cross-matched the lists of reference star positions using the STARLINK TOPCAT software. Subsequently, we employed routines in the STARLINK SLALIB library to construct six co-efficient linear transforms between the two images of the putative systems, where $>3\sigma$ outliers were iteratively clipped from the fits. The proper motions, in pixels, were determined by taking the differences between the observed and calculated locations of candidates in the second-epoch imaging. These were then converted into milliarcseconds per year in right ascension and declination using the world coordinate systems of the first-epoch data sets and dividing by the time baseline between the two observations, ∼4.08 yr for System 1 and ∼47.95 yr for System 2 (Table 1). The uncertainties on these measurements were estimated from the dispersion observed in the (assumed near-zero) proper motions of stars of comparable brightness surrounding each system. The relative proper motion vector point diagrams for the objects (solid triangles) are shown in Fig. 1.

Inspection of these plots reveals that our proper motion measurements of the components of the pairs are significant at $>3\sigma$ and consistent with each other within their 1σ uncertainties. For each case we estimated the probability that this similarity could have occurred merely by chance. We selected all spectroscopically confirmed white dwarfs within 10° of these systems from the SDSS DR4 white dwarf catalogue (Eisenstein et al. 2006) that met the photometric selection criteria outlined in Section 2.1. We cross-correlated these with the SSS database to obtain their proper motions. After cleaning these samples for objects with poorly constrained astrometry (e.g. $\chi^2 > 3$ or flagged as bad and/or proper motion uncertainties >7.5 mas yr^{-1}), we are left with 59 and 159 white dwarfs in the general directions of System 1 and System 2, respectively. An examination of this astrometry reveals that none and seven sources in

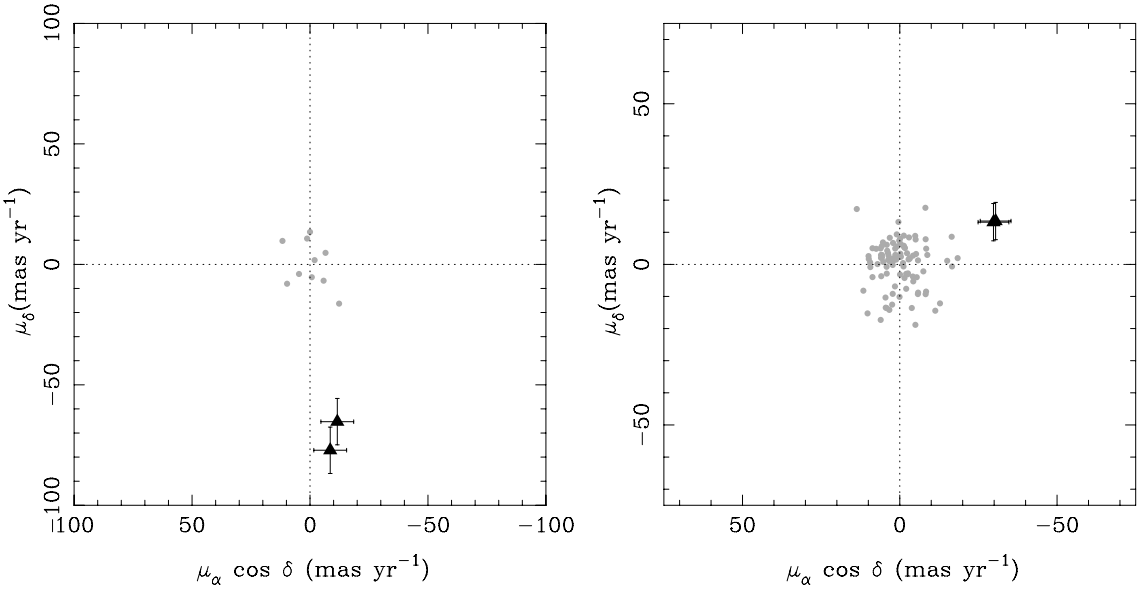

Figure 1. A vector point diagram of the relative proper motions of the SDSS J092647.00+132138.4 + J092646.88+132134.5 system (left) and the SDSS J150746.48+521002.1 + J150746.80+520958.0 system (right). The reference stars used in the construction of the linear transform are also shown (light grey points). The similarities between the proper motions of the components of these putative binary systems are clear to see (solid triangles).

these samples have proper motions that could be deemed as consistent (within 2σ of the mean proper motion of the components of the putative system) with System 1 and System 2, respectively. Therefore we estimate the probabilities that the proper motions of these objects are similar by chance are less than 0.02 and 0.05 respectively. Combined with the likelihoods of chance projected angular proximity we find that the probabilities of these two systems merely being optical doubles are less than $P \sim 0.0006$ and $P \sim 0.0015$, giving a potent argument in favour of their association.

3 SPECTROSCOPIC ANALYSIS

3.1 Follow-up optical spectroscopy of the binary components

We obtained the optical spectroscopy of System 1 in visitor mode with the ESO VLT and the Focal Reducer and low-dispersion Spectrograph (FORS2). A full description of the FORS2 instrument can be found on the ESO webpages.[1] These observations (1 × 360-s and 1 × 500-s exposures) were conducted on the night of 2010 February 6 when the seeing was good but there was some cirrus scattered across the sky. All data were acquired using the 2 × 2 binning mode of the *E2V* CCD, the 600B+24 grism and a 1.3-arcsec slit, which gives a notional resolution of $\lambda/\Delta\lambda \sim 600$. The components of System 2 were observed with the William Herschel Telescope (WHT) and the double-armed Intermediate dispersion Spectrograph and Imaging System (ISIS) on the night of 2008 July 24. These observations were conducted when the sky was photometric, with seeing ∼0.6–0.9 arcsec. The spectrograph was configured with a 1.0-arcsec slit and with the R300B ($\lambda/\delta\lambda \approx 2000$) and the R1200R ($\lambda/\delta\lambda \approx 10\,000$) gratings on the blue and red arms, respectively. Three 1800-s exposures covering the two wavelength ranges, $\lambda \approx 3600$–5200 Å and 6200–7000 Å, were obtained simultaneously.

The CCD frames were debiased and flat-fielded using the IRAF procedure CCDPROC. Cosmic-ray hits were removed using the routine

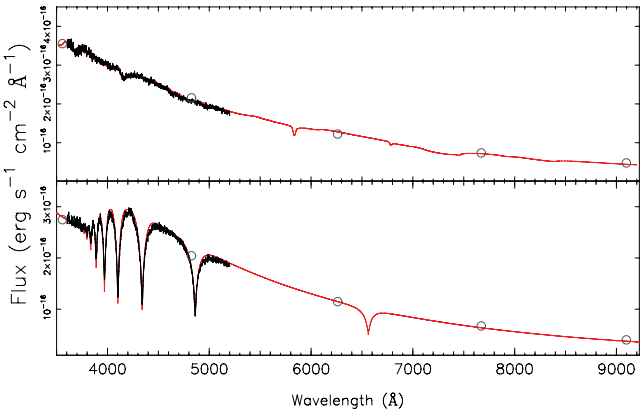

Figure 2. VLT + FORS2 spectroscopy of SDSS J092646.88+132134.5 (upper) and SDSS J092647.00+132138.4 (lower) with SDSS *u*, *g*, *r*, *i* and *z* fluxes (open grey circles) and synthetic spectra (red line) overplotted. The spectrum of SDSS J092647.00+132138.4 is clearly that of an H-rich white dwarf, while that of SDSS J092646.88+132134.5 displays several weaker features that are consistent with magnetically broadened and shifted Balmer lines.

LACOS SPEC (van Dokkum 2001). Subsequently, the spectra were extracted using the APEXTRACT package and the wavelength calibrated by comparison with a CuAr+CuNe arc spectrum taken immediately before and after the science exposures (ISIS) or with a He+HgCd arc spectrum obtained within a few hours of the science frames (FORS2). The removal of the remaining instrument signature from the science data was undertaken using observations of the bright DC white dwarfs WD1918+386 (ISIS) and LHS2333 (FORS2). The spectra of the components of System 1 and System 2 are shown in Figs 2 and 3.

3.2 Effective temperatures and surface gravities

The optical energy distributions of SDSS J092647.00+132138.4 (hereafter DA1) and SDSS J150746.48+521002.1 (hereafter DA2)

[1] http://www.eso.org/instruments/fors2/

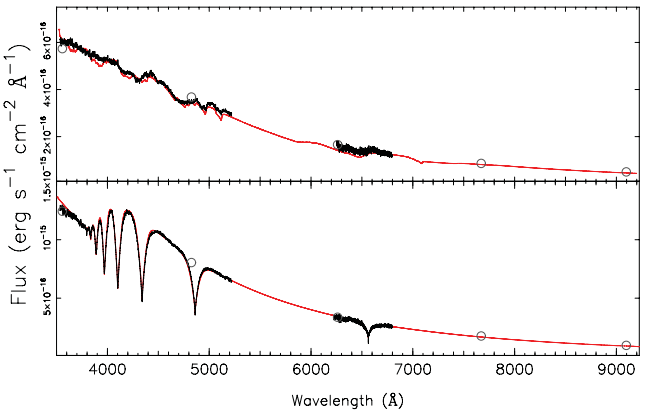

Figure 3. WHT + ISIS spectroscopy of SDSS J150746.48+521002.1 (lower) and SDSS J150746.80+520958.0 (upper) with SDSS *u*, *g*, *r*, *i* and *z* fluxes overplotted (open grey circles). The spectrum of SDSS J150746.48+521002.1 is clearly that of an H-rich white dwarf, while that of SDSS J150746.80+520958.0 displays several weaker features that are consistent with magnetically broadened and shifted Balmer lines.

each display broadened H-Balmer line series, and these objects are unmistakably hydrogen-rich white dwarfs. In contrast, no prominent features at the notional wavelengths of the lines of either H I or He I are observed in the spectra of SDSS J092646.88+132134.5 (hereafter, DAH1) and SDSS J150746.80+520958.0 (hereafter, DAH2). However, neither data set is completely smooth like the spectrum of a DC white dwarf; instead, they display a number of shallow depressions across the observed wavelength range reminiscent of a H-rich HFMWD such as SDSS J172045.37+561214.9 (Gänsicke, Euchner & Jordan 2002).

To determine the effective temperatures and the surface gravities of DA1 and DA2 we compared the observed Balmer lines, H8 to Hβ, with a grid of synthetic profiles (e.g. Bergeron, Saffer & Liebert 1992). These are based on recent versions of the plane-parallel, hydrostatic, local thermodynamic equilibrium (LTE) atmosphere and spectral synthesis codes ATM and SYN (e.g. Koester 2010), which include an updated physical treatment of the Stark broadening of H I lines (Tremblay & Bergeron 2009). The fitting procedure was performed with the spectral analysis package XSPEC (Shafer 1991). XSPEC folds a model through the instrument response before comparing the result with the data by means of a χ^2-statistic. The best model representation of the data is found by incrementing free grid parameters in small steps, linearly interpolating between points in the grid, until the value of χ^2 is minimized. Formal errors in the '$T_{\rm eff}$'s and 'log g's are calculated by stepping the parameter in question away from its optimum value and redetermining the minimum χ^2 until the difference between this and the true minimum χ^2 corresponds to 1σ for a given number of free model parameters (e.g. see Lampton, Margon & Bowyer 1976). It is important to be aware that these errors do not take into account shortcomings in the models or systematic issues affecting the data (e.g. flaws in the flat-fielding), so they undoubtedly underestimate the true uncertainties in the parameters. Therefore in our subsequent analysis we assume more realistic levels of uncertainty of 2.3 per cent and 0.07 dex in effective temperature and surface gravity, respectively (e.g. see Napiwotzki, Green & Saffer 1999). The results of our line fitting are shown in Table 2. Synthetic colours for H-rich white dwarfs at these effective temperatures and surface gravities (e.g. Holberg & Bergeron 2006) appear to be broadly consistent with the SDSS photometry for DA1 and DA2 (Table 1).

The energy distributions of the DAH components DAH1 and DAH2 were compared with a grid of model spectra for HFMWDs. These were calculated with a radiative transfer code for magnetized, high-gravity atmospheres. The code calculates both theoretical flux (Stokes *I*) and polarization (Stokes *V*) spectra, for a given temperature and pressure structure ($T_{\rm eff}$, log g) and a specific magnetic field vector with respect to the line of sight and the normal on the surface of the star (see Jordan 1992; Jordan & Schmidt 2003). However, as no polarization information is available from our data sets, our analysis was limited to the flux spectra (Stokes parameter *I*). For computational efficiency, we made use of our existing three-dimensional grid of synthetic spectra. This grid spans the effective temperature range $7000 \leq T_{\rm eff} \leq 50\,000$ K in 14 steps, treats magnetic field strengths in the range 1 MG $\leq B \leq$ 1.2 GG in 1200 steps, and has 17 values of the field direction ψ relative to the line of sight as the independent variables (9 entries, equally spaced in cos ψ). All spectra were calculated for a surface gravity of log $g = 8$ (see Külebi et al. 2009). Limb darkening is accounted for by a simple linear scaling law (see Euchner et al. 2002).

The magnetic field geometry of the DAHs was determined using a modified version of the code developed by Euchner et al. (2002). This code calculates the total flux distribution for an arbitrary magnetic field topology by adding appropriately weighted synthetic spectra for a large number of surface elements and then evaluates the goodness of fit. We used a simple model for the magnetic geometry, namely a dipole with an offset on its polar axis. This is the most parameter-efficient way of generating non-dipolar geometries and is representative of dipole plus quadrupole configurations. Moreover, these models are ubiquitous in the diagnosis of single-phase HFMWD spectra (Külebi et al. 2009). The resulting magnetic parameters of our fits are summarized in Table 3. As explained in Euchner et al. (2002), these values might not be unique and it is possible to fit similar spectra with different models. However, this analysis is fully satisfactory in the context of this work as we are interested in a good spectral model of a given object for determining the temperature. We find that the magnetic field geometries of these two HFMWDs are quite different. While the field of DAH1 does not deviate significantly from dipolarity, in the case of DAH2 the offset parameter is quite large and the magnetic field distribution used in the construction of the fitted spectrum departs substantially from a simple dipole, with field strengths of between 45 and 317 MG.

Table 2. Effective temperatures, surface gravities, predicted absolute *r* magnitudes, distance moduli, masses and cooling times for the DA components of the two wide binary systems.

SDSS	$T_{\rm eff}^{*}$	log g^{*}	M_r	$r - M_r$	$M(\mathrm{M}_{\odot})$	τ_c (Myr)
J092647.00+132138.4	10482^{+47}_{-47}	$8.54^{+0.03}_{-0.03}$	$12.57^{+0.17\ddagger}_{-0.17}$	$5.89 \pm 0.18\ddagger$	$0.79 \pm 0.06\ddagger$	$833^{+123\ddagger}_{-123}$
J150746.48+521002.1	17622^{+99}_{-94}	$8.13^{+0.02}_{-0.02}$	$11.38^{+0.11}_{-0.11}$	5.91 ± 0.11	0.70 ± 0.04	147^{+24}_{-21}

*Formal fit errors.

‡ Adjusted to account for spectroscopic overestimate of mass.

Table 3. Effective temperatures, field strengths and geometries, masses and cooling times for the magnetic components of the two binary systems.

SDSS	$T_{\rm eff}$	$B_{\rm dip}$ (MG)	$z_{\rm off}$ ($R_{\rm WD}$)	Inclination (°)	M ($M_\odot$)	τ_c (Myr)
J092646.88+132134.5	9500 ± 500	210 ± 25.1	-0.09 ± 0.01	21.8 ± 7.9	0.62 ± 0.10	726^{+140}_{-107}
J150746.80+520958.0	18000 ± 1000	65.2 ± 0.3	-0.39 ± 0.03	36.4 ± 4.1	0.99 ± 0.05	321^{+47}_{-40}

After obtaining a satisfactory representation of the magnetic field structures, the effective temperature of each star was assessed from the line strengths and the continuum (e.g. Gänsicke et al. 2002). These are also shown in Table 3. While in some cases the magnetic analysis can be hindered by the lack of a realistic and easily applicable theory for the simultaneous impact of Stark and Zeeman effect on the spectral lines, this is not a problem for the field strengths relevant to this work ($B > 50$ MG).

3.3 White dwarf masses and cooling times

We used our measurements of the effective temperatures and the surface gravities of DA1 and DA2, in conjunction with the evolutionary models of Fontaine, Brassard & Bergeron (2001), to estimate their masses and cooling times. For consistency with our previous work and a large number of other recent studies (e.g. Dobbie et al. 2009; Williams, Bolte & Koester 2009; Kalirai et al. 2008; Liebert, Bergeron & Holberg 2005a), we adopted calculations that include a mixed CO core and a thick H surface-layer structure. It is important to note that DA1 has an effective temperature of $T_{\rm eff} < 12\,000$ K. Spectroscopic mass determinations are known to be systematically larger in this regime than at higher effective temperatures, where they agree well with those derived from gravitational redshifts (e.g. Bergeron, Wesemael & Beauchamp 1995; Reid 1996). This trend probably arises from shortcomings in the treatment of convection within the model atmosphere calculations (Koester 2010). Based on the studies of Tremblay, Bergeron & Gianninas (2011), Koester et al. (2009) and Kepler et al. (2007), we estimated the size of this effect at $T_{\rm eff} = 10\,500$ K to be $\Delta M = +0.16 \pm 0.04\,{\rm M}_\odot$. The properties reported in Table 2 reflect a downward adjustment of this size to the estimated mass of DA1. We used the grids of synthetic photometry of Bergeron et al. (1995), which were updated by Holberg & Bergeron (2006), to derive the absolute r magnitudes of DA1 and DA2 and to determine the distance moduli of their host binary systems (Table 2). We neglected foreground extinction in these directions, as dust maps suggest $A_V < 0.1$ integrated along these sight lines through the Galaxy (Schlegel, Finkbeiner & Davis 1998).

To evaluate the masses of DAH1 and DAH2, we first assumed that they reside at the same distance as their non-magnetic companions. We then determined the radius of each HFMWD through scaling its distance by the square root of the estimated flux ratio, $(f/F)^{0.5}$, where f is the observed flux at the Earth's surface and F is the flux at the surface of the white dwarf. The surface flux in the SDSS filters (r, i and z; e.g. Fukugita et al. 1996) for each object was derived from the non-magnetic, pure-H model white dwarf atmospheres of Holberg & Bergeron (2006), where cubic splines were used to interpolate between points in this grid. Next we used the mass–radius relations for non-magnetic DA white dwarfs predicted by the evolutionary models of Fontaine et al. (2001) to obtain estimates of the masses for DAH1 and DAH2 of $M = 0.62 \pm 0.10\,{\rm M}_\odot$ and $M = 0.99 \pm 0.05\,{\rm M}_\odot$, respectively. Finally, we used the evolutionary models to determine their cooling times to be $\tau_{\rm cool} = 726^{+140}_{-107}$ Myr and $\tau_{\rm cool} = 321^{+47}_{-40}$ Myr, respectively. The uncertainties in all derived parameters here were determined using a Monte Carlo-like approach in which we created 25 000 realizations of each binary system under the assumption that the adopted errors on the effective temperatures (2.3 per cent), the surface gravities (0.07 dex) and the observed magnitudes (Table 1) of the component stars are normally distributed. We also noted that the SDSS magnitudes (Table 1) have an absolute precision of 2 per cent (Adelman-McCarthy et al. 2008).

4 THE PROGENITORS OF THE HFMWDS

4.1 In wide double-degenerate systems

From their observed positions on the sky and the distance moduli in Table 2, we determined that the components of System 1 and System 2 have minimum separations of $a \sim 650$ au and $a \sim 750$ au, respectively. Even assuming that the original orbital separations of these binaries were substantially smaller (e.g. Valls-Gabaud 1988), the Roche lobes of their components have probably always been much larger than the dimensions of an asymptotic giant branch (AGB) star ($r \lesssim 4$ –5 au; Iben & Livio 1993). Thus this work doubles the number of known wide, magnetic + non-magnetic double-degenerate binaries in which, through their large orbital separations, the components could be expected to have evolved essentially as single stars.

Intriguingly, in three of the four pairings now known, the non-magnetic component has a substantially greater mass than the value observed at the prominent peak in the field white dwarf mass distribution (e.g. $M \sim 0.6\,{\rm M}_\odot$; Bergeron et al. 1992; Kepler et al. 2007). The intermediate temperatures ($T_{\rm eff} = 10\,500$–$16\,000$ K) of these three non-magnetic white dwarfs, coupled with their comparatively high masses, link their HFMWD companions to an early-type stellar population. For example, DA2 has a mass of $M \approx 0.66$–$0.74\,{\rm M}_\odot$ and a corresponding cooling time of $\tau \approx 126$–171 Myr. Assuming it has evolved essentially as a single object from a star with an initial mass of $M_{\rm init} \approx 2.3$–$3.7\,{\rm M}_\odot$ (e.g. Williams et al. 2009; Kalirai et al. 2008; Dobbie et al. 2006), allowing for a stellar lifetime as predicted by the solar metallicity model grid of Girardi et al. (2000), the total age of the binary is likely to be $\tau \lesssim 1150$ Myr. Thus the formation of DA2 appears to be associated with a star of initial mass $M_{\rm init} > 2.2\,{\rm M}_\odot$. Following a similar line of reasoning, from the mass and cooling time of DA1 we infer the age of the host system to be $\tau \lesssim 1300$ Myr, which corresponds to the lifetimes of stars with initial masses $M_{\rm init} > 2.1\,{\rm M}_\odot$.

Owing to our adopted colour-selection criteria, our search for wide double-degenerate binaries is sensitive only to relatively recently formed white dwarfs. For example, a $0.6\,{\rm M}_\odot$ white dwarf cools to $T_{\rm eff} \sim 9000$ K ($g - r \approx 0.0$; Holberg & Bergeron 2006) in only 800 Myr. Assuming single-star evolution, a massive white dwarf companion to a degenerate formed from a sufficiently long-lived progenitor ($M_{\rm init} \lesssim 1.6\,{\rm M}_\odot$) will generally always have cooled below our photometric colour limits before the latter has formed. Thus the detection of systems in which the components

have quite different evolutionary time-scales is not favoured. If HFMWDs are frequently associated with relatively short main-sequence lifetimes, we might expect in a 'blue' colour-selected survey a low probability of finding them paired with white dwarfs that have 'average' masses ($M \sim 0.6\,M_{\odot}$). Interestingly, the DA in the fourth pairing that lies within the SDSS DR7 footprint but that failed our survey selection criteria on the grounds of one component being too red (the DAH) has a comparatively low mass, $M = 0.54\,M_{\odot}$. The large difference of ∼1.6 Gyr between the cooling times of PG 1258+593 and SDSS J130033.48+590407.0 means that, within the measurement uncertainties, this HFMWD could still be the progeny an early-type star with $M_{\rm init} \approx 2$–$3\,M_{\odot}$ (Girven et al. 2010).

4.2 In closer or less well-characteriszed systems

Three further hot ($T_{\rm eff} \gtrsim 9000$ K) magnetic + non-magnetic binaries have been identified, and spectroscopically confirmed, to date (the DAH component of G 62-46 has only $T_{\rm eff} \sim 6000$ K). The components of at least one of these systems, LB 11146 (PG 0945+245), are separated by only $a \sim 0.6$ au (Nelan 2007). As this is less than the radius of an AGB star, it is likely they interacted during prior phases of their evolution. Detailed analysis of this binary has revealed it to consist of a $T_{\rm eff} \sim 14\,500$ K, $M \approx 0.9\,M_{\odot}$ DA and a similarly hot, massive magnetic white dwarf with a field strength $B \gtrsim 300$ MG (Liebert et al. 1993). 2RE J1440+750 (EUVE J1439+75.0) has been shown, through a detailed spectroscopic (and imaging) analysis, to consist of a $M \sim 0.9\,M_{\odot}$ DA and a $M \sim 1.0\,M_{\odot}$ DAH ($B \sim$ 14–16 MG), each having $T_{\rm eff} > 20\,000$ K, and with a projected orbital separation of $a \lesssim 250$ au (Vennes et al. 1999). CBS 229 was identified as an unresolved DA+DAH binary during the course of a spectroscopic survey of bright white dwarfs ($V \leq 17.5$) drawn from the catalogue of McCook & Sion (1999). Gianninas et al. (2009) performed a preliminary analysis of a composite spectrum of this pair and found that the non-magnetic component has $T_{\rm eff} \approx 15\,000$ K and $\log g \approx 8.5$, corresponding to a mass of $M \approx 0.9\,M_{\odot}$. The shape of their deblended spectrum of the DAH suggests that the two objects have similar effective temperatures. Our examination of the SDSS imaging reveals that the components are in fact resolved into two photocentres with a projected separation of ∼1.3 arcsec (see Fig. 4, left). From the Gianninas et al. (2009) parameters for the DA and its magnitude from the SDSS z imaging (the band in which the objects are most clearly resolved), we provisionally estimate a distance to this binary of $d \sim 140$ pc and a projected orbital separation of $a \sim 180$ au. Thus CBS 229 appears to be a wide magnetic + non-magnetic double-degenerate system

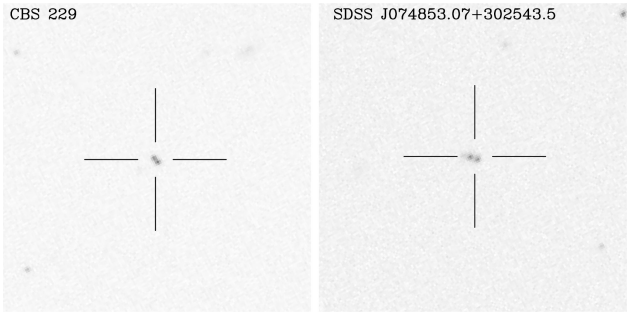

Figure 4. SDSS z-band image of two candidate spatially resolved magnetic + non-magnetic double-degenerate systems, CBS 229 (Gianninas, Bergeron & Ruiz 2009) and SDSS J074853.07+302543.5. Images are approximately 1×1 arcmin^2 with N at the top and E to the left.

that escaped detection by our survey. This is probably because of the u-band magnitude measurement for the NE component, which appears to be anomalous.

Although it is possible that past mass exchange within at least the first of these binaries has influenced the characteristics of their white dwarfs, as is observed in three out of four of the confirmed wide systems, the non-magnetic components in each of LB 11146, EUVE J1439+75.0 and, provisionally, CBS 229 also appear to have substantially greater masses than is typical of field degenerates. This is consistent with their magnetic white dwarf companions being related to an early-type stellar population.

5 COOLING TIMES OF THE HFMWDS AND CANONICAL STELLAR EVOLUTION

5.1 The DAH SDSS J150746.80+520958.0

DA2 has a mass and cooling time that are comparable to those of several degenerate members of the Hyades (e.g. WD 0352+098, WD 0421+162; Claver et al. 2001). This suggests that the host binary system is likely to have a total age that is similar to that of this cluster ($\tau = 625 \pm 50$ Myr, Perryman et al. 1998). We made detailed estimates of this age using our determinations of the progenitor masses of DA2 and DAH2 (obtained from three recent, independent, derivations of the IFMR), the stellar lifetimes as predicted by the solar metallicity models of Girardi et al. (2000) and by assuming standard single-star evolution (Table 4). We find that our estimates are only formally consistent within their quoted (1σ) error bounds when the oldest, least well constrained of the three approximations to the IFMR (Dobbie et al. 2006) is adopted. When either of the two other IFMRs is assumed, the age derived from the HFMWD is lower than that obtained from the DA.

This discord is not statistically significant alone, but it is notable for being in the same sense as seen for RE J0317-853 (Ferrario et al. 1997) and the Praesepe cluster HFMWD, EG 59 (Claver et al. 2001). It has been proposed that the age paradox of the RE J0317-853 + LB 9208 system is attributable to the former component having formed through the merging of the white dwarf progenies of two stars of more modest initial mass (than is assumed in the case of single-star evolution). This could also explain why this HFMWD is observed to rotate with a relatively short period of only 725 s (Ferrario et al. 1997). More recently, Külebi et al. (2010) argued that the cooling time of this HFMWD appears at odds with that of LB 9208 only because the mass of the former has been slightly underestimated (∼5 per cent) owing to the fact that evolutionary models neglect the effects of the magnetic field on the structure of the white dwarf. However, our revised calculations suggest that this earlier conclusion is erroneous and that these structural effects are unable to account fully for the age discrepancy. In Külebi et al. (2010), the tables of Holberg & Bergeron (2006) were extrapolated to estimate the new cooling ages but effectively considered the wrong radii and hence incorrect luminosities for the cooling. Here we instead consider a simple approach using Mestel's equation (see Shapiro & Teukolsky 1983) for a half-carbon, half-oxygen white dwarf, which is a good approximation especially before the onset of crystallization (equation 2):

$$\tau_{\rm cool} \approx 1.1 \times 10^{7} \left(\frac{M}{M_{\odot}}\right)^{5/7} \left(\frac{L}{L_{\odot}}\right)^{-5/7} \text{ years}, \qquad (2)$$

where $\tau_{\rm cool}$ is the cooling age, M is the mass of the star in solar masses and L is its luminosity in solar luminosiies. Given that the luminosity is constant, any difference in mass (ΔM) causes an

Table 4. Progenitor masses and system age estimates for the components of the DA+DAH system SDSS J150746.48+521002.1 + SDSS J150746.80+520958.0. These are based on three recent estimates of the form of the IFMR, namely 1, Dobbie et al. (2006); 2, Kalirai et al. (2008); 3, Williams et al. (2009); and on stellar lifetimes from the solar metallicity evolutionary models of Girardi et al. (2000).

Component	IFMR 1		IFMR 2		IFMR 3	
SDSS	$M_{\rm init}$ ($M_\odot$)	System age (Myr)	$M_{\rm init}$ ($M_\odot$)	System age (Myr)	$M_{\rm init}$ ($M_\odot$)	System age (Myr)
J150746.48+521002.1	$3.06^{+0.66}_{-0.58}$	599^{+357}_{-181}	$2.76^{+0.50}_{-0.47}$	753^{+390}_{-217}	$2.76^{+0.37}_{-0.36}$	754^{+259}_{-167}
J150746.80+520958.0	$5.30^{+0.86}_{-0.75}$	426^{+67}_{-44}	$5.50^{+0.62}_{-0.59}$	416^{+55}_{-38}	$5.07^{+0.41}_{-0.42}$	437^{+52}_{-37}

underestimation of cooling age, linearly (equation 3):

$$\frac{\Delta\tau_{\rm cool}}{\tau_{\rm cool}} = \frac{5}{7}\frac{\Delta M}{M}. \quad (3)$$

Hence if the mass of RE J0317-853 is underestimated by ∼5 per cent, the underestimation of the cooling age would be only ∼3.5 per cent, which is far smaller than the observed ∼30 per cent.

It should be noted that our calculation is based on the assumption that the radius is inflated by 8–10 per cent. It is possible that the stellar interior contains a higher level of magnetic energy, which might have an even stronger influence on the structure, especially if this approaches 10 per cent of the gravitational binding energy as suggested by Ostriker & Hartwick (1968). However, this supposition is not based on quantitative considerations of the stellar structure. Recently, Reisenegger (2009) investigated the magnetic structure of non-barotropic stars and put an upper limit on the internal magnetic energy that can be supported. This value is limited by the entropy of the star. For white dwarfs it is sufficient to consider only the ions, and hence entropy is directly related to the core temperature. A 1.1 $M_\odot$ white dwarf with an effective temperature of 18 000 K can support a magnetic energy of at most ∼2.4 per cent of its gravitational binding energy. In this case the radius is 16 per cent larger, which corresponds to that of a 1.0 $M_\odot$ non-magnetic white dwarf. Thus the most extreme mass underestimation expected for DAH2 is 10 per cent, which translates to a cooling age increase of only ∼7 per cent, compared with an observed discrepancy of perhaps ∼50 per cent.

5.2 The DAH SDSS J092646.88+132134.5

We have similarly estimated the progenitor masses of DA1 and DAH1 and calculated the total age of this other new binary, under the assumption of standard single-star evolution. These two sets of estimates, which are shown in Table 5, are not formally consistent within their 1σ errors for any of our three adopted IFMRs. However, as in the case of our other binary system, the discrepancy is not overwhelming, statistically. The variance suggested here is in the opposite sense to that observed for the three HFMWDs discussed previously, with DAH1 appearing too old for its mass or, alternatively, too low in mass for its cooling time. It could be expected, on the basis of single-star evolution, that because the white dwarfs in this system have similar cooling times, they should have comparable masses, having descended from stars with similar initial masses and lifetimes. DAH1 may have endured greater mass loss than assumed for a single star. This could be a consequence of its having a close companion. Studies of stellar multiplicity have revealed that at least 10 per cent of stars are members of triple or higher-order systems (Raghavan et al. 2010; Abt & Levy 1976). For reasons of dynamical stability, these systems are frequently hierarchically structured, with triples often consisting of a body in a relatively wide orbit around a much closer pairing (Harrington 1972). DA1 and DAH1 perhaps trace what was the wider orbit of a putative triple system, with the latter object possibly having been (or perhaps still being) part of a tighter pairing. A $M_{\rm init} \sim 3.5\,M_\odot$ star that experiences Roche lobe overflow around the time of central helium ignition can lead to the formation of a CO white dwarf with a mass towards the lower end of the range estimated for this HFMWD (e.g. Iben & Tutukov 1985). However, we note that an observed lack of HFMWDs with close detached companions (Liebert et al. 2005b) has been one of the main arguments that these stars are formed through close binary interaction (Tout et al. 2008). Whether or not this mechanism was required for the manufacture of either of the two HFMWDs identified in this work, the parameters of their DA companions argue that they are associated with an early-type stellar population.

The sizeable uncertainties associated with the parameters of the HFMWDs highlight the need to expand substantially the sample of those that are members of either nearby star clusters or wide binary systems so that we can begin to firmly identify any trends in their cooling times and inferred progenitor masses, relative to non-magnetic white dwarfs. For now, a relatively straightforward but useful exercise would involve photometrically monitoring these two new systems to search for short-period variability that may reveal evidence that more closely links their evolution and that of the RE J0317-853 + LB 9208 system.

6 THE SPACE VELOCITY OF SDSS J150746.48+521002.1

We exploited the higher-resolution spectroscopy we have in hand for DA2 to determine the radial velocity of this system from the

Table 5. Progenitor masses and system age estimates for the components of the DAH+DA system SDSS J092647.00+132138.4 + J092646.88+132134.5. These are based on three recent estimates of the form of the IFMR, namely 1, Dobbie et al. (2006); 2, Kalirai et al. (2008); 3, Williams et al. (2009); and on stellar lifetimes from the solar metallicity evolutionary models of Girardi et al. (2000).

Component	IFMR 1		IFMR 2		IFMR 3	
SDSS	$M_{\rm init}$ ($M_\odot$)	System age (Myr)	$M_{\rm init}$ ($M_\odot$)	System age (Myr)	$M_{\rm init}$ ($M_\odot$)	System age (Myr)
J092647.00+132138.4	$3.73^{+0.78}_{-0.69}$	1092^{+202}_{-94}	$3.61^{+0.63}_{-0.65}$	1115^{+178}_{-58}	$3.48^{+0.47}_{-0.51}$	1146^{+134}_{-42}
J092646.88+132134.5	$2.49^{+0.92}_{-0.85}$	1531^{+1334}_{-372}	$2.08^{+0.96}_{-0.92}$	2072^{+4464}_{-781}	$2.18^{+0.77}_{-0.77}$	1892^{+2215}_{-549}

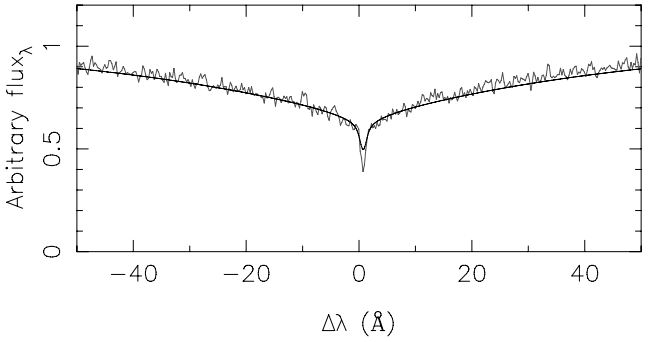

Figure 5. The results of our fitting of a synthetic profile (black line) to the central portions of the observed Hα Balmer line of SDSS J150746.48+521002.1 (grey line). The flux$_\lambda$ units are arbitrary.

observed shift of the Hα line core. We removed the effects of telluric water vapour from our red-arm ISIS data using a template absorption spectrum. The observed Hα line and the profile from a non-LTE synthetic spectrum corresponding to $T_{\rm eff} = 17\,500$ K and $\log g = 8.15$, generated using TLUSTY (v200; Hubeny 1988; Hubeny & Lanz 1995) and SYNSPEC (v49; Hubeny, I. and Lanz, T. 2001, http://nova.astro.umd.edu/), were both normalized using a custom-written IDL routine. The model was then compared with the data, allowing a velocity parameter to vary freely[2] and using a Levenberg–Marquardt algorithm to minimize a χ^2 goodness-of-fit statistic. The result of this process is displayed in Fig. 5, and the line-velocity shift, after correction to the heliocentric rest frame, is shown in Table 6. This measurement is not sensitive to the details of the model we adopt for effective temperatures and surface gravities within plausible limits. The uncertainty we quote was estimated using the bootstrapping method of statistical resampling (Efron 1982). Subsequently, the gravitational redshift (v in km s^{-1}) component of this velocity shift was derived using equation (4), where M and R are the mass and the radius of the white dwarf in solar units, respectively:

$$v = 0.635 M/R. \quad (4)$$

As described above, the mass and radius of DA2 were determined using the evolutionary tracks of Fontaine et al. (2001). The radial velocity was then derived from the difference between the measured shift of the line and the calculated gravitational redshift (Table 6). Finally, adopting the mean of our new (relative)[3] proper-motion measurements for the components of this binary ($\mu_\alpha \cos\delta = 30.7 \pm 3.5$ mas yr^{-1}, $\mu_\delta = 12.9 \pm 4.1$ mas yr^{-1}), we followed the prescription outlined by Johnson & Soderblom (1987) to calculate the heliocentric space velocity of DA2 to be $U = -20.6 \pm 3.0$ km s^{-1}, $V = -20.8 \pm 2.8$ km s^{-1} and $W = -6.4 \pm 4.6$ km s^{-1}. This is coincident with the space velocity of the oldest component of the Pleiades moving group, B3, identified by Asiain et al. (1999) in their *Hipparcos* kinematic analysis of the B-, A- and F-type stars in the vicinity of the Sun. The subpopulations of this supercluster are estimated to span the range of ages $\tau \approx 60$–600 Myr (Eggen 1992). While this result is not definitive proof of an association between System 2 and the Pleiades moving group, it is at least in accord with our conclusions above, from the cooling time and the inferred main-sequence lifetime of the DA component, that this is a relatively young binary.

[2] An additional flux-scaling parameter was allowed to vary by up to 1 per cent.

[3] The difference between relative and absolute values are comparable to or smaller than the quoted errors on the proper motion.

7 SUMMARY AND FUTURE WORK

Within a broader photometric, astrometric and spectroscopic survey for wide double-degenerate systems (Baxter et al. in prep.) we have discovered two new binaries, each containing a hydrogen-rich HFMWD and a non-magnetic (DA) component. We used synthetic spectra generated from offset dipole magnetic models to estimate the field strengths for DAH1 and DAH2 to be $B_{\rm dip} \sim 210$ MG ($z_{\rm off} \sim -0.09 R_{\rm WD}$) and $B_{\rm dip} \sim 65$ MG ($z_{\rm off} \sim -0.39 R_{\rm WD}$), respectively. Our measurements of the effective temperatures and surface gravities of their non-magnetic companions allow us to infer the masses of these DAHs to be $M = 0.62 \pm 0.10\,{\rm M}_\odot$ and $M = 0.99 \pm 0.05\,{\rm M}_\odot$, respectively. If we assume that the two components in each of these systems evolved essentially as single stars we find a mild discord in their cooling times, with DAH2 appearing slightly too hot and young relative to expectations, while DAH1 appears to be 'too old' for its mass or, alternatively, too low in mass for its cooling time. The former object may represent the third known HFMWD that is apparently 'too young', perhaps hinting at a trend, although the study of more such systems is required to confirm this possibility. The latter white dwarf may have been part of a hierarchical triple system and have suffered greater mass loss than expected of a single star during its earlier evolution.

In three of the four wide systems that are now known, the non-magnetic components have larger masses than is typical of field white dwarfs. The characteristics (i.e. masses, cooling times and kinematics) of the DAs in our two new binaries argue that their HFMWD companions are members of relatively young systems and are therefore associated with early-type stars ($M_{\rm init} \gtrsim 2\,{\rm M}_\odot$). The non-magnetic components in three additional but spatially unresolved, young, magnetic + non-magnetic binaries known prior to this work (at least one of which is a physically close system in which the components may have previously exchanged mass), also have atypically large masses. This is consistent with the HFMWDs in these systems also being related to an early-type stellar population. To reinforce these findings and to delineate clearly any trends in the cooling times of HFMWDs that could shed light on their formation and on the impact of magnetic fields on stellar evolution, an enlarged sample of these objects that are located either in wide double-degenerate binaries or in nearby open clusters will be required. As a starting point we have flagged the previously known DA+DAH system CBS 229 as a probable wide binary. In addition, we note that the SDSS spectrum of one component of the close ($\sim$1.6 arcsec) pair of relatively bright ($g \sim 17.6$ mag), blue point sources SDSS J074853.07+302543.5 and SDSS J074852.95+302543.4 (Fig. 4) displays a Zeeman-split, pressure-broadened Balmer line series and thus also represents a promising candidate for a wide double-degenerate system containing a DAH.

ACKNOWLEDGMENTS

This work was based on observations made with ESO telescopes at the La Silla and Paranal observatories under program ID 084.D-1097. The WHT is operated on the island of La Palma by the Isaac Newton Group in the Spanish Observatorio del Roque de los Muchachos of the Instituto de Astrofsica de Canarias. Funding for SDSS and SDSS-II was provided by the Alfred P. Sloan Foundation, the Participating Institutions, the National Science Foundation, the US

Table 6. Additional parameters of the DA component SDSS J150746.48+521002.1, including the radial velocity and the heliocentric space velocity.

SDSS	$M_{\rm WD}$ ($M_\odot$)	$R_{\rm WD}$ ($R_\odot \times 10^{-3}$)	Hα shift	v	$rv_{\rm WD}$	U ($\rm km\,s^{-1}$)	V	W
J150746.48+521002.1	0.695 ± 0.043	11.9 ± 0.6	$19.1^{+2.8}_{-4.1}$	37.1 ± 4.0	$-18.0^{+4.9}_{-5.7}$	-20.6 ± 3.0	-20.8 ± 2.8	-6.4 ± 4.6

Department of Energy, the National Aeronautics and Space Administration, the Japanese Monbukagakusho, the Max Planck Society, and the Higher Education Funding Council for England. The SDSS website is http://www.sdss.org/. The SDSS is managed by the Astrophysical Research Consortium for the Participating Institutions. The Participating Institutions are the American Museum of Natural History, the Astrophysical Institute Potsdam, the University of Basel, the University of Cambridge, Case Western Reserve University, the University of Chicago, Drexel University, Fermilab, the Institute for Advanced Study, the Japan Participation Group, Johns Hopkins University, the Joint Institute for Nuclear Astrophysics, the Kavli Institute for Particle Astrophysics and Cosmology, the Korean Scientist Group, the Chinese Academy of Sciences (LAMOST), Los Alamos National Laboratory, the Max-Planck-Institute for Astronomy (MPIA), the Max-Planck-Institute for Astrophysics (MPA), New Mexico State University, Ohio State University, the University of Pittsburgh, the University of Portsmouth, Princeton University, the United States Naval Observatory, and the University of Washington. BK acknowledges support from MICINN grant AYA08-1839/ESP, ESF EUROCORES Program EuroGENESIS (MICINN grant EUI2009-04170), 2009SGR315 of the Generalitat de Catalunya and EU-FEDER funds. NL acknowledges funding from Spanish Ministry of Science and Innovation through the national program AYA2010-19136.

REFERENCES

Abt H. A., Levy S. G., 1976, ApJS, 30, 273
Adelman-McCarthy J. K. et al., 2008, ApJS, 175, 297
Angel J. R. P., Borra E. F., Landstreet J. D., 1981, ApJS, 45, 457
Asiain R., Figueras F., Torra J., Chen B., 1999, A&A, 341, 427
Barstow M. A., Jordan S., O'Donoghue D., Burleigh M. R., Napiwotzki R., Harrop-Allin M. K., 1995, MNRAS, 277, 971
Bergeron P., Saffer R. A., Liebert J., 1992, ApJ, 394, 228
Bergeron P., Ruiz M.-T., Leggett S. K., 1993, ApJ, 407, 733
Bergeron P., Wesemael F., Beauchamp A., 1995, PASP, 107, 1047
Bertin E., Arnouts S., 1996, A&AS, 117, 393
Bowyer S., Lampton M., Lewis J., Wu X., Jelinsky P., Malina R. F., 1996, ApJS, 102, 129
Burleigh M. R., Jordan S., Schweizer W., 1999, ApJ, 510, L37
Casewell S. L., Dobbie P. D., Napiwotzki R., Burleigh M. R., Barstow M. A., Jameson R. F., 2009, MNRAS, 395, 1795
Claver C. F., Liebert J., Bergeron P., Koester D., 2001, ApJ, 563, 987
Dobbie P. D. et al., 2006, MNRAS, 369, 383
Dobbie P. D., Napiwotzki R., Burleigh M. R., Williams K. A., Sharp R., Barstow M. A., Casewell S. L., Hubeny I., 2009, MNRAS, 395, 2248
Efron B., 1982, Society of Industrial and Applied Mathematics CBMS-NSF Monographs, 38
Eggen O. J., 1992, AJ, 103, 1302
Eisenstein D. J. et al., 2006, ApJS, 167, 40
Euchner F., Jordan S., Beuermann K., Gänsicke B. T., Hessman F. V., 2002, A&A, 390, 633
Ferrario L., Vennes S., Wickramasinghe D. T., Bailey J. A., Christian D. J., 1997, MNRAS, 292, 205
Finley D. S., Koester D., 1997, ApJ, 489, L79
Fontaine G., Brassard P., Bergeron P., 2001, PASP, 113, 409
Fukugita M., Ichikawa T., Gunn J. E., Doi M., Shimasaku K., Schneider D. P., 1996, AJ, 111, 1748
Gänsicke B. T., Euchner F., Jordan S., 2002, A&A, 394, 957
Gianninas A., Bergeron P., Ruiz M. T., 2009, J. Phys. Conf. Ser., 172, 012021
Girardi L., Bressan A., Bertelli G., Chiosi C., 2000, A&AS, 141, 371
Girven J., Gänsicke B. T., Külebi B., Steeghs D., Jordan S., Marsh T. R., Koester D., 2010, MNRAS, 404, 159
Hambly N. C. et al., 2001, MNRAS, 326, 1279
Harrington R. S., 1972, Celest. Mech., 6, 322
Holberg J. B., Bergeron P., 2006, AJ, 132, 1221
Hubeny I., 1988, Comput. Phys. Comm., 52, 103
Hubeny I., Lanz T., 1995, ApJ, 439, 875
Iben I., Jr, Livio M., 1993, PASP, 105, 1373
Iben I., Jr, Tutukov A. V., 1985, ApJS, 58, 661
Johnson D. R. H., Soderblom D. R., 1987, AJ, 93, 864
Jordan S., 1992, A&A, 265, 570
Jordan S. et al., 1998, A&A, 330, 277
Jordan S., Schmidt H., 2003, in Hubeny I., Mihalas D., Werner K., eds, ASP Conf. Ser. Vol. 288, Stellar Atmosphere Modelling. Astron. Soc. Pac., San Francisco, p. 625
Kalirai J. S., Hansen B. M. S., Kelson D. D., Reitzel D. B., Rich R. M., Richer H. B., 2008, ApJ, 676, 594
Kawka A., Vennes S., Wickramasinghe D. T., Schmidt G. D., Koch R., 2003, in de Martino D., Silvotti R., Solheim J.-E., Kalytis R., eds, NATO ASIB Proc. 105, White Dwarfs. Kluwer, Dordrecht, p. 179
Kawka A., Vennes S., Schmidt G. D., Wickramasinghe D. T., Koch R., 2007, ApJ, 654, 499
Keller S. C. et al., 2007, Proc. Astron. Soc. Aust., 24, 1
Kepler S. O., Kleinman S. J., Nitta A., Koester D., Castanheira B. G., Giovannini O., Costa A. F. M., Althaus L., 2007, MNRAS, 375, 1315
Koester D., 2010, Mem. Soc. Astron. Ital., 81, 921
Koester D., Voss B., Napiwotzki R., Christlieb N., Homeier D., Lisker T., Reimers D., Heber U., 2009, A&A, 505, 441
Külebi B., Jordan S., Euchner F., Gänsicke B. T., Hirsch H., 2009, A&A, 506, 1341
Külebi B., Jordan S., Nelan E., Bastian U., Altmann M., 2010, A&A, 524, A36
Lampton M., Margon B., Bowyer S., 1976, ApJ, 208, 177
Liebert J., Bergeron P., Schmidt G. D., Saffer R. A., 1993, ApJ, 418, 426
Liebert J., Bergeron P., Holberg J. B., 2003, AJ, 125, 348
Liebert J., Bergeron P., Holberg J. B., 2005a, ApJS, 156, 47
Liebert J. et al., 2005b, AJ, 129, 2376
McCook G. P., Sion E. M., 1999, ApJS, 121, 1
Monet D. G. et al., 2003, AJ, 125, 984
Munn J. A. et al., 2004, AJ, 127, 3034
Napiwotzki R., Green P. J., Saffer R. A., 1999, ApJ, 517, 399
Nelan E. P., 2007, AJ, 134, 1934
Ostriker J. P., Hartwick F. D. A., 1968, ApJ, 153, 797
Perryman M. A. C. et al., 1998, A&A, 331, 81
Pye J. P. et al., 1995, MNRAS, 274, 1165
Raghavan D. et al., 2010, ApJS, 190, 1
Reid I. N., 1996, AJ, 111, 2000
Reisenegger A., 2009, A&A, 499, 557
Roeser S., Demleitner M., Schilbach E., 2010, AJ, 139, 2440
Schlegel D. J., Finkbeiner D. P., Davis M., 1998, ApJ, 500, 525
Shafer R. A., Haber L. F., Arnaud K. A., Tennant A. F., 1991, XSPEC Users Guide ESA TM-09, Paris

Shapiro S. L., Teukolsky S. A., 1983, Black Holes, White Dwarfs, and Neutron Stars: The Physics of Compact Objects. Wiley, New York
Struve F. G. W., 1852, in Stellarum Fixarum Imprimus Compositarum Positiones Mediae pro Epocha 1830.0, Academia Caesareae Petropolitanae, Petrograd
Tout C. A., Wickramasinghe D. T., Liebert J., Ferrario L., Pringle J. E., 2008, MNRAS, 387, 897
Tremblay P., Bergeron P., 2009, ApJ, 696, 1755
Tremblay P., Bergeron P., Gianninas A., 2011, ApJ, 730, 128
Valls-Gabaud D., 1988, Ap&SS, 142, 289
Vennes S., Ferrario L., Wickramasinghe D. T., 1999, MNRAS, 302, L49
van Dokkum P. G., 2001, PASP, 113, 789
Weidemann V., 2000, A&A, 363, 647
Wickramasinghe D. T., Ferrario L., 2005, MNRAS, 356, 1576
Williams K. A., Bolte M., Koester D., 2009, ApJ, 693, 355
York D. G. et al., 2000, AJ, 120, 1579

This paper has been typeset from a TEX/LATEX file prepared by the author.